論文 한국정밀공학회지 제8권 제2호 1991. 6
Journal of the Korean Society of precision Engineering Vol. 8. No. 2 June. 1991.

얇은 림 평치차의 이뿌리 응력 계산법

정 태 형*, 최 재 훈**

A Root Fillet Stress Calculation Method for Thin-Rimmed Spur Gears

Tae Hyong CHONG, Jae Hoon CHOI

Abstract

A method to apply the approximation formulae[1] for tooth fillet and root stresses of a thin-rimmed rack to the calculation of stress state of thin-rimmed external and internal spur gears is introduced. The stress values by the method proposed in this paper have shown good agreement with those by the FEM analysis and also by the stress measurement of strain survey investigation. By this method, reliable stress state at tooth fillet and root areas in the thin-rimmed external and internal spur gears can be easily calculated, and a practical design method for the bending strength of such thin-rimmed gears is established.

초 록

얇은 림 랙의 이뿌리응력 계산식을 얇은 림 외접 및 내접치차의 이뿌리응력 계산에 응용하는 방법을 도입하여 이뿌리응력 계산법을 확립하였다. 이 계산법에 따른 이뿌리 응력값은 유한요소법(FEM) 해석 및 스트레인 게이지에 의한 실측치와 잘 일치함을 밝혔다. 따라서 본 논문에서 제안한 계산법에 의해 얇은 림 외접 및 내접치차의 이뿌리 부위의 응력을 신뢰성 높게 계산할 수 있게 되었으며, 굽힘강도에 기초를 둔 실제적인 설계법을 확립하였다.

* Department of Mechanical Engineering, Hanyang University (한양대학교 기계공학과)
** Samsung Engineering(삼성 엔지니어링)

Keywords : Gear(치차), Thin-Rimmed Spur Gears(얇은 림 평치차), Root Fillet Stress Calculation Method(이뿌리응력 계산법), Design Method(설계법)

Nomenclature

b : face width
c_k : bottom clearance
d : width of bottom of tooth space
h : whole depth of tooth
h_p1 : tooth depth from loading position P1 to critical section of tooth
m : module
r : radius of mean circle of equivalent rim of thin-rimmed gear
r_r : radius of root circle of gear
s_p1 : chordal tooth thickness at loading position P1
s_F : chordal tooth thickness at critical section
t : rim thickness
t_e : equivalent rim thickness
x : addendum modification coefficient
x_c : addendum modification coefficient in cutter
x_i : addendum modification coefficient in internal gear
z : number of teeth
z_c : number of teeth in cutter
z_i : number of teeth in internal gear
F_i : internal forces
H : distance from the mean circle of equivalent rim to root circle of a thin-rimmed gear
K : stiffness matrix
L : distance from the loading position to the mean circle of the equivalent rim along the tooth center line
P_n : load
α : pressure angle
ρ : radius of curvature of tooth fillet
ρ_a : radius of rounding of tip on cutter
ϕ : angle to designate a position of the bottom of tooth space or a position of tooth on the rim
ϕ_0 : central angle between nodes

ω : loading angle on tooth flank (the complementary angle for the angle between tooth cener line and the line of action on tooth flank)

θ : tangential angle (angle between tooth center line and the tangent to tooth fillet curve) to designate a position at tooth fillet and root areas

$\sigma(\theta)$: actual stress distribution and its magnitude at the position θ at tooth fillet and root areas

$\sigma_t(\theta)$: stress components of actual stress distribution

$\sigma_{t.nom}$: nominal stresses defined at the critical section of tooth and at the cross section of rim

1. Introduction

The state of stress at the tooth fillet and root areas of thin-rimmed gears (i, e., thin-rimmed external, internal gears and rack) seems different from that of solid gears because of large deformation of the thin rim. A lot of research has been published[1-16] on the tooth fillet and root stresses of such thin-rimmed gears. A general calculation formula for the tooth fillet and root stresses has, however, not been obtained yet, and it becomes significantly difficult to work out the bending strength calculation for such thin-rimmed gears. To develop the bending strength calculation method of such thin-rimmed gears, a set of approximation formulae for the calculation of the tooth fillet and root stress distribution of a thin-rimmed rack were derived[1] from the results of many FEM analyses. In this paper, this approximate calculation method is applied to the calculation of the tooth fillet and root stresses of thin-rimmed external and internal spur gears, which are fixed by spokes and bolts and supported by pinned coupling similar to geared coupling. The reliability and capability of the calculation method proposed in the present paper is examined by the comparison of stress values obtained from this calculation method with those from the FEM calculation and also with the strain survey investigation. A design method for the bending strength of the thin-rimmed external and internal gears is described.

2. Application method of the approximation stress formulae to thinrimmed spur gears.

The tooth fillet and root stresses of thin-rimmed spur gears are influenced by the geometry of tooth form and gear body, loading condition on tooth flank, and supporting conditions of the gear, etc. ; the distributions and the magnitudes of stresses at tooth fillet and root areas of a thin-rimmed spur gear can be calculated by the approximation formulae already derived[1] : Eqs. (1)~(4)

$$\sigma(\theta)=\sum_{i=(a)}^{(f)}\sigma_i(\theta),\quad 1=(a),\ \cdots,\ (f) \tag{1}$$

$$\sigma_i(\theta)=(A_1\theta^3+A_2\theta^2+A_3\theta+A_4)\sigma_{i\cdot nom} \tag{2}$$

$$A_1=B_{1i}S^3+B_{2i}S^2T+B_{3i}ST^2+B_{4i}T^3+ +B_{5i}S^2+B_{6i}ST+B_{7i}T^2+B_{8i}S +B_{9i}T+B_{10i} \tag{3}$$

$$S=0.1(s_F/\rho),\quad T=0.1(t/\rho). \tag{4}$$

methods (boundary conditions) of the thin-rimmed gear is considered by the nominal stresses of rim which appear at the cross section of the thin-rimmed gear ($\sigma_{(d)nom}$, $\sigma_{(e)nom}$, $\sigma_{(f)nom}$). The former 3 nominal stresses of tooth at the critical section can be easily obtained by simple consideration of tooth

Table 1 The values of coefficients A_i and B_{ji}

for stress component	B_{ji} / A_i	B1i	B2i	B3i	B4i	B5i	B6i	B7i	B8i	B9i	B10i
$\sigma_{(a)}(\theta)$	A1	0.1868	0.1424	-0.6379	0.1917	-1.3585	2.4053	-0.4578	-0.2591	-0.6955	2.3180
	A2	-0.8473	-0.2305	2.0945	-0.8091	5.3016	-8.8757	2.5594	0.4562	0.6635	-6.3258
	A3	1.0845	-0.0302	-1.8799	0.9714	-6.1152	9.0098	-3.6615	0.9436	1.4223	3.3808
	A4	-0.3126	-0.0894	0.3521	-0.3462	1.8958	-1.3353	1.3593	-2.1284	-1.2730	1.6254
$\sigma_{(b)}(\theta)$	A1	0.2673	-5.7444	2.3881	-3.9081	9.7032	7.8069	15.7366	-22.0673	-28.3284	25.7134
	A2	-1.9383	18.6058	-7.6689	12.5287	-26.8121	-25.9919	-49.7557	66.5725	88.7455	-79.4101
	A3	3.2617	-18.5263	7.9246	-12.8521	21.2401	25.0307	50.4025	-58.6969	-87.6421	73.9576
	A4	-1.5128	5.4080	-2.7137	3.9972	-4.1367	-5.4413	-15.5893	12.2824	26.1241	-18.3672
$\sigma_{(c)}(\theta)$	A1	0.3655	-0.9218	0.0451	-0.0318	-0.0406	3.1892	-0.2759	-3.7370	-1.1378	3.6523
	A2	-1.0656	3.5478	-0.7172	0.0910	-1.6231	-10.1119	1.8559	16.0303	0.6084	-13.2737
	A3	0.7988	-3.9218	1.4375	-0.0879	3.9352	8.5824	-2.8251	-19.7806	3.3036	14.0271
	A4	0.0066	0.6983	-0.3390	-0.0206	-1.7018	-1.1776	0.7225	5.2598	-1.0315	-3.3872
$\sigma_{(d)}(\theta)$	A1	0.2225	-0.1840	-0.0370	-0.7931	-0.9099	0.7304	3.4874	1.5676	-5.6424	0.5196
	A2	-0.9175	0.6881	0.2903	2.2467	3.8661	-3.3922	-9.9699	-6.0022	16.7452	-2.3729
	A3	1.1217	-0.9062	-0.4776	-1.8273	-4.5659	4.9418	8.1076	5.8940	-14.3624	4.1745
	A4	-0.2958	0.4022	0.0699	0.4311	0.8002	-1.5446	-1.8206	-0.3042	3.3032	-1.4195
$\sigma_{(e)}(\theta)$	A1	0.1931	-0.1946	-0.0062	0.4596	-0.7343	0.7966	-2.5303	0.7581	3.9979	-4.7973
	A2	-0.6682	0.4952	0.0910	-1.9652	3.0365	-2.4925	10.2018	-4.4715	-15.8097	15.6538
	A3	0.7043	-0.3480	-0.1035	2.6622	-3.6605	2.1601	-13.2523	6.7919	20.3354	-15.1151
	A4	-0.1527	0.1011	-0.0333	-1.0964	0.7590	-0.3493	5.3051	-1.4589	-8.0797	4.8203
$\sigma_{(f)}(\theta)$	A1	-0.6294	3.8093	0.6164	2.1790	-3.6879	-13.5460	-8.7069	20.0825	16.4098	-13.2669
	A2	1.4308	-12.7030	-1.7298	-5.8289	15.1932	43.8744	21.7471	-70.8828	-41.1713	35.6949
	A3	-0.5483	12.0913	2.3017	4.3347	-17.8994	-43.1852	-15.3446	73.2989	29.7858	-28.2001
	A4	-0.3750	-2.5038	-1.5236	-0.6530	5.6203	11.5341	2.9441	-17.9756	-6.6693	6.3046

The values of coefficients A_i and B_{ji} in Eqs. (2) and (3) are as shown in Table 1. When applying these approximation stress formulae to thin-rimmed spur gears with dimensions as shown in Fig. 1, the influence of geometry of tooth form is considered by the nominal stresses of the tooth which appear at the critical section of the tooth ($\sigma_{(a)nom}$, $\sigma_{(b)nom}$, $\sigma_{(c)nom}$ in Eq. (2)) just the same as in the case for a solid gear tooth. The influence of radius of curvature of rim, rim rigidity and supporting geometry and loading poition on tooth flank. A general method to calculate the later 3 nominal stresses of rim appearing at the rim cross section of the thin-rimmed gear with various dimensions, which is supported by different methods is shown in the following sections.

3. Equivalent rim thickness of the thin-rimmed spur gear

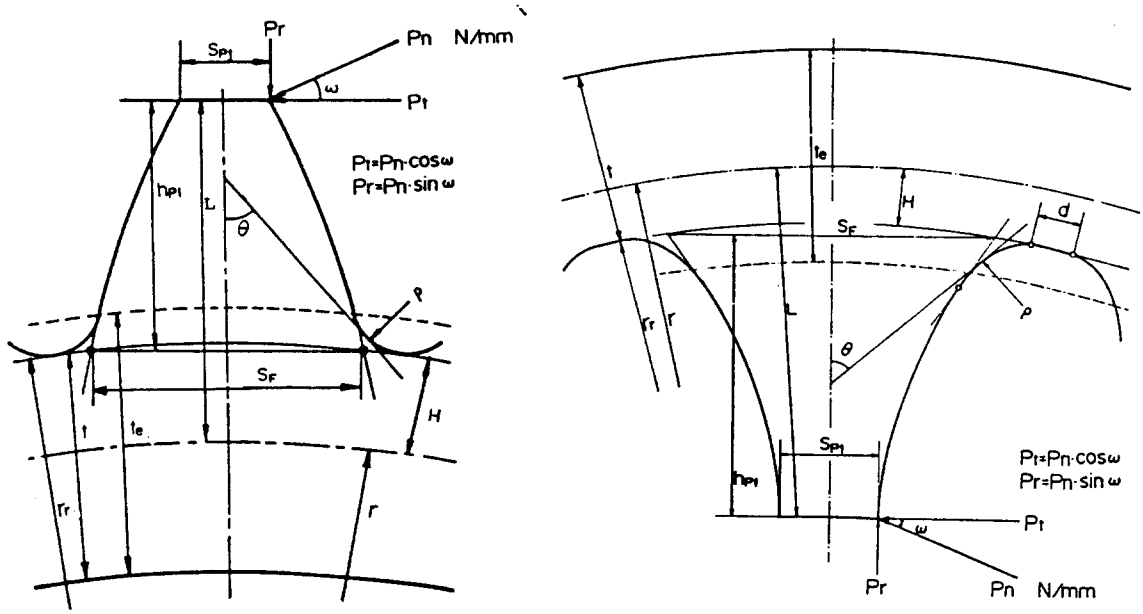

(a) External gear (b) Internal gear

Fig.1 Notations to show dimensions of tooth and rim of thin- rimmed spur gears and a loading condition for calculating tooth fillet and root stresses.

In order to obtain the nominal stresses appearing at the rim cross section of the thin-rimmed gear, the gear-toothed rim of the thin-rimmed gear is regarded here as a ring with equivalent rigidity. The rim thickness of this equivalent ring t_e (cf. Fig. 1) by Sinkevich[17] and Dinovichi[18] is here employed. The mean radius r of the equivalent ring and the equivalent rim thickness t_e are expressed by

$$r = r_r \mp 0.5(t \mp m(A_{oe} - A_{te})) \quad (5)$$

$$t_e = t + m(A_{oe} + A_{te}) \quad (6)$$

$$\left.\begin{aligned} A_{te} &= 0.19[1 + c_k/m + \{2 + 17(c_k/m)\}/z] + (0.01x + x/z) \\ A_{oe} &= 0.19[1 + c_k/m - \{2 + 17(c_k/m)\}/z] + (0.02x + x/z) \end{aligned}\right\} \quad (7)$$

where, the signs - (upper sign) and + (lower sign) in Eq. (5) are for the thin-rimmed external and internal gears, and A_{oe} and A_{te} are the coefficients for the thin-rimmed external and internal gears, respectively.

4. Relation between force and displacement in the rim of thin-rimmed spur gear.

In order to obtain nominal stresses at the cross section of rim of the thin-rimmed gear, it is necessary to calculate, at first, the displacements and internal forces which occur at the rim section of the thin-rimmed gear owing to applied load. The gear-toothed rim of thin-rimmed gear, i. e., the rim with the equivalent rigdity is taken for a ring made from an ensemble of continuous curved beams as shown in Fig. 2. The nodes in this figure

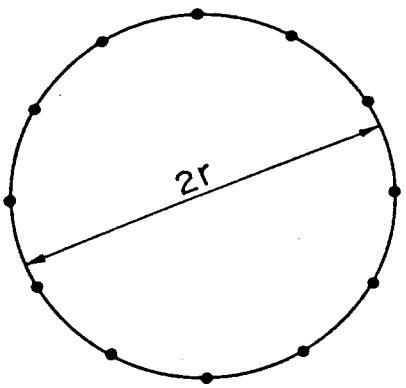

Fig.2 Continuous curved beam model of a thin-rimmed gear and the nodes of curved beam.

are, in general, the load acting points and/or supporting points of the thin-rimmed gear. Let the notations U_{ri}, U_{hi}, U_{mi} denote the displacements in the radial, circumferential, rotational directions respectively. Their signs are taken plus in the direction of the arrow shown in Fig. 3. The notations W_{ri}, W_{hi}, W_{mi} denote the external forces in the same directions. And here the expression is used

$$\mathbf{U}_i=\begin{bmatrix} U_{ri} \\ U_{hi} \\ U_{mi} \end{bmatrix}, \quad \mathbf{W}_i=\begin{bmatrix} W_{ri} \\ W_{hi} \\ W_{mi} \end{bmatrix}, \tag{8}$$

for a definite node i. Expressing $\mathbf{F}_{li}$, and $\mathbf{F}_{ri}$ as the internal forces acting on the free end of the curved beam fixed at the left end shown in Fig. 4 and the internal forces on the free end of the curved beam fixed at the right end shown in Fig. 5 respectively, the internal forces and displacements between node i and node i-1 and those between node i and node i+1 are expressed by

$$\begin{aligned} \mathbf{F}_{li} &= B_l^{-1}\mathbf{U}_i - B_l^{-1}C_l\mathbf{U}_{i-1} \\ \mathbf{F}_{ri} &= B_r^{-1}\mathbf{U}_i - B_r^{-1}C_r\mathbf{U}_{i+1} \end{aligned} \tag{9}$$

The relation between the external force W_i acting on node i and the displacements at continuous 3 nodes i-1, i, i+1, is expressed by

$$B_1\mathbf{U}_{i-1} + B_2\mathbf{U}_i + B_3\mathbf{U}_{i+1} = \mathbf{W}_i . \tag{10}$$

In Eqs. (9) and (10)

$$\begin{aligned} &B_l = -B_l^{-1}C_l, \quad B_2 = B_l^{-1} + B_r^{-1}, \\ &B_3 = -B_r^{-1}C_r, \end{aligned} \tag{11}$$

$$B_l = \frac{r^3}{EI}\begin{bmatrix} b_{11} & b_2 & b_{13} \\ b_{21} & b_2 & b_{23} \\ b_{31} & b_2 & b_{33} \end{bmatrix},$$

$$b_{11} = 0.5(1+k_e)(\phi_0 - \sin\phi_0\cos\phi_0),$$

$$b_{12} = \mp 0.5\{(\cos\phi_0 - 1)^2 - k_e\sin^2\phi_0\},$$

$$b_{13} = \mp(1-\cos\phi_0),$$

$$b_{22} = 0.5\{(3\phi_0 - 4\sin\phi_0 + \sin\phi_0\cos\phi_0) + k_e(\phi_0 + \sin\phi_0\cos\phi_0)\},$$

$$b_{23} = \phi_0 - \sin\phi_0,$$

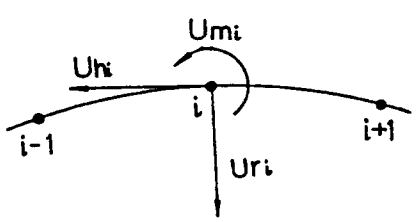

(a) External gear

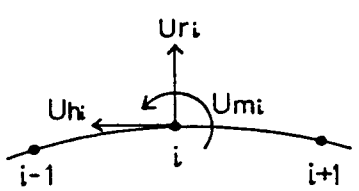

(b) Internal gear

Fig.3 Displacements in the radial, circumferential, and rotational directions at node i.

$b_{33}=\phi_0$,

$b_{21}=b_{12}$, $b_{31}=b_{13}$, $b_{32}=b_{23}$,

$$B_r^{-1}=\begin{bmatrix}1&0&0\\0&-1&0\\0&0&-1\end{bmatrix}B_l^{-1}\begin{bmatrix}1&0&0\\0&-1&0\\0&0&-1\end{bmatrix},$$

$$C_l=\begin{bmatrix}\cos\phi_0 & \pm\sin\phi_0 & \mp\sin\phi_0\\ \mp\sin\phi_0 & \cos\phi_0 & 1-\cos\phi_0\\ 0 & 0 & 1\end{bmatrix},$$

$$C_r=\begin{bmatrix}1&0&0\\0&-1&0\\0&0&-1\end{bmatrix}C_l\begin{bmatrix}1&0&0\\0&-1&0\\0&0&-1\end{bmatrix},$$

$k_e=(1/3)(t_e/2r)^2+(1/5)(t_e/2r)^4+$
$+(1/7)(t_e/2r)^6+\cdots\cdots$,

$$\bar{U}=\begin{bmatrix}U_1\\ \vdots\\ U_i\\ \vdots\\ U_n\end{bmatrix},\quad \bar{W}=\begin{bmatrix}W_1\\ \vdots\\ W_i\\ \vdots\\ W_n\end{bmatrix}, \tag{12}$$

and we have Eq. (13) for the relation between force and displacement where K

$$\bar{W}=K\,\bar{U}\ , \tag{13}$$

represents the stiffness matrix.

Generalizing the expressions mentioned above to the case of a curved beam which has many nodes and no node is fixed, the relation between forces and displacements at each node can be expressed from Eq. (13) by Eq. (14).

In this case the stiffness matrix K in Eq. (14) is a $(3n \times 3n)$ matrix with 3 kinds of matrix elements B_1, B_2, B_3.

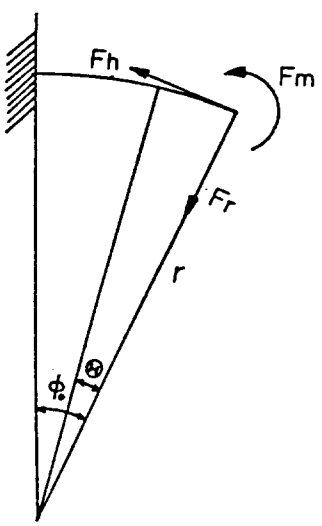

Fig.4 A curved beam on which a force acts at the node at right end when the node at left end is fixed.

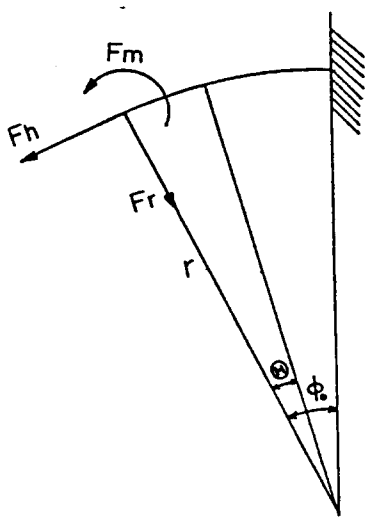

Fig.5 A curved beam on which a force acts at the node at left end when the node at right end is fixed.

where, the upper and lower signs − and + represent the thin-rimmed external and internal gears, respectively. Using the expression for the displacements and external forces for n numbers of nodes are obtained al Eq. (12),

$$\begin{bmatrix} W_1 \\ W_2 \\ W_3 \\ \vdots \\ W_{n-1} \\ W_n \end{bmatrix} = \begin{bmatrix} B_2 & B_3 & 0 & 0 & \cdots\cdots & 0 & B_1 \\ B_1 & B_2 & B_3 & 0 & \cdots\cdots & 0 & 0 \\ 0 & B_1 & B_2 & B_3 & \cdots\cdots & 0 & 0 \\ \vdots & \vdots & \vdots & \vdots & & \vdots & \vdots \\ 0 & 0 & 0 & 0 & \cdots\cdots & B_2 & B_3 \\ B_3 & 0 & 0 & 0 & \cdots\cdots & B_1 & B_2 \end{bmatrix} \begin{bmatrix} U_1 \\ U_2 \\ U_3 \\ \vdots \\ U_{n-1} \\ U_n \end{bmatrix} \quad (14)$$

When a thin-rimmed spur gear is supported by bolts or spokes and/or similar method, in a practical calculation, it is easier to calculate the stiffness matrix K by making the displacement of the node i corresponding to a supporting point equal to zero, i. e., $\mathbf{U}_i = 0$. When a thin-rimmed internal gear is supported by geared coupling and/or similar method, the elastic supporting conditions at geared coupling part of the internal gear is taken into consideration, i. e., the geared coupling teeth on the periphery of the internal gear are considered to be simple plate springs.

On the other hand referring to Fig. 1, the external force $\mathbf{W}_i$ for loaded tooth of the thin-rimmed spur gear is

$$\mathbf{W}_i = \begin{bmatrix} P_n \sin\omega \\ P_n \cos\omega \\ \pm(LP_n\cos\omega - 0.5 s_{p1} P_n \sin\omega) \end{bmatrix} \quad (15)$$

and $W_i = 0$ for all other teeth out of meshing, and the signs + and − are for the thin-rimmed external and internal gears. The displacement $\mathbf{U}_i$ at each node can be calculated by introducing Eq. (15) into Eq. (14), and the internal force $\mathbf{F}_i$ is obtained by substituting the resultant data $\mathbf{U}_i$ into Eq. (9).

5. Calculation of nominal stresses

Fig. 6 shows 6 nominal stresses $\sigma_{i.\,nom}$ (i=

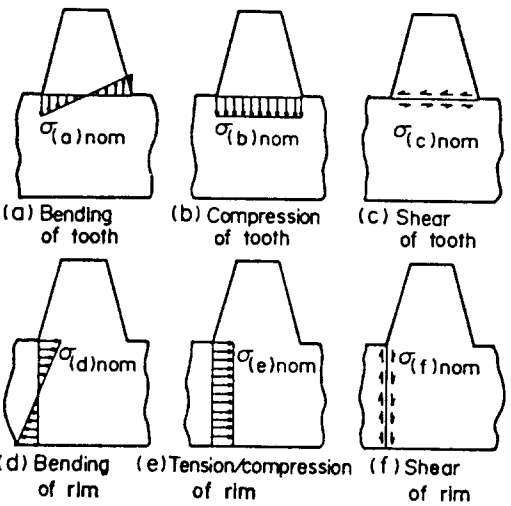

Fig. 6 Nominal stresses of a thinrimmed spur gear.

(a), ……, (f)) necessary to calculate the stress state at tooth fillet and root areas of thin-rimmed spur gears. Among these nominal stresses, the nominal bending, compressive, shearing stresses of tooth stress occurring at the critical section of a loaded tooth are obtained from the same method as the case of solid gear tooth; the nominal bending, tensile/compressive, shearing stresses of rim stress occurring at the cross section of rim of the thin-rimmed spur gear can be obtained by use of the internal force $\mathbf{F}_i$, of an equivalent curved beam, calculated by Eq. (9). The nominal stresses of the thin-rimmed spur gear for unit face width are expressed by the following equations :

nominal bending stress of tooth:

$$\sigma_{(a)nom} = \pm 6\,(P_n/s_F^2)\,(h_{P1}\cos\omega - 0.5 s_{p1}\sin\omega) \quad (16)$$

nominal compressive stress of tooth:

$$\sigma_{(b)nom} = -P_r/s_F = -P_n\sin\omega/s_F \quad (17)$$

nominal shearing stress of tooth:

$$\sigma_{(c)nom} = \pm P_t/s_F = \pm P_n\cos\omega/s_F \quad (18)$$

nominal bending stress of rim:

$$\sigma_{(d)nom} = (F_m/tr)[1 \pm H/\{\varkappa(r \pm H)\}] \quad (19)$$

nominal tensile/compressive stress of rim:

$$\sigma_{(e)nom} = F_h/t \quad (20)$$

nominal shearing stress of rim:

$$\sigma_{(f)nom} = F_r/t \quad (21)$$

where, κ is the number defined as, in the curved beam, $\varkappa = (1/3)(t/2r)^2 + (1/5)(t/2r)^4 + (1/7)(t/2r)^6 + \cdots$, the signs + and - in Eqs. (16) and (18) are used in calculating stresses on the tension side and compression side respectively, and the signs + (upper) and - (lower) in Eq. (19) represent the thin-rimmed external and internal gears respectively.

6. Compaison between tooth fillet and root stress values obtained from the proposed method and those from the FEM calculation and also from the stress measurement.

6.1 For a thin-rimmed external spur gear

To examine the accuracy of the proposed calculation method in the present paper for a thin-rimmed spur gear, the tooth fillet and root stress calculations were carried out for a thin-rimmed spur gear, the tooth fillet and root stress calculations were carried out for a lot of kinds of external gears : They are standard addendum spur gears of module m= 4㎜, h=2, 25m, z=36, 60, 72, 90, 120, t= 1. 5m(6㎜), 2m(8㎜), 3m(12㎜), 4m(16㎜), 5m (20㎜), 6m(24㎜), 8m(32㎜). The tooth forms are generated by cutting with rack cutters of α=20, 22. 5, 25 degs., x_c=0, and ρ_a=0. 375m. The boundary condition is supporting the thin-rimmed external gears by 6 spokes at the same intervals of rim spans. The unit normal load (Pn/b=9. 8N/㎜) is applied on the tip of central tooth between supporting spokes under a single tooth pair meshing, and the fillet and root stresses of the loaded tooth are calculatd by the FEM and by the proposed calculation method mentioned to date.

Fig. 7 shows the comparison of both calculated results. The point of tensile fillet stress is θ=30deg. and that of compressive root stress is θ=60deg. It is recognized from this figure that the stress values obtained by the FEM calculations and those by the present calculation method show fairly good agreement in the cases of (a) and (b), even if the number of teeth and rim thicknes$ of the thin-rimmed external spur gear are different from each other. These results show that this calculation method for the tooth fillet and root stresses has high accuracy as the same degree as the accuracy of the FEM calculation. In comparison with the results for the cases of z=60~120, with decreasing rim thickness, the tooth fillet and root stresses of the case when the gear has a lot of number of teeth(z=120) are smaller on the tension side but larger on the compression side than those of the cases when the number of teeth

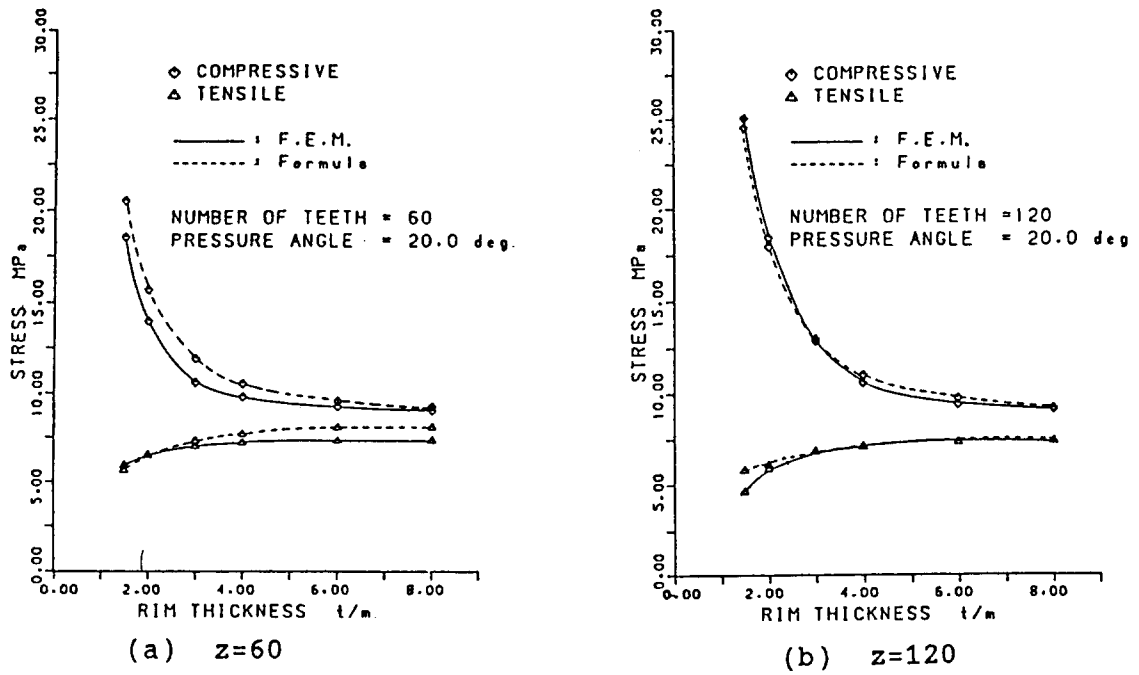

Fig.7 Comparison between tooth fillet and root stresses obtained by the present stress calculation method (dotted line) and those by the FEM calculation (line) according to the variation of rim thickness and number of teeth.

becomes smaller. This comes from the differences of the radius of curvature of rim and the rigidity of rim owing to the different length of span of the rim between spokes, although the thin-rimmed external gear is supported by the same numbers of spokes(6 spokes). But when the rim is thicker than 5m, the tooth fillet and root stresses are almost same in each case as those of gears with thick rims. In each case, with decreasing rim thickness, tensile stresses become a little smaller and compressive stresses become sharply larger. In the case of z=120 and t/m =2, the ratio between compressive stress and tensile stress becomes almost 3 times. It is seen from these comparisons that the influences of supporting conditions (boundary conditions) on the tooth fillet and root stresses calculation method.

Fig. 8 shows the comparison of tooth fillet and root stresses obtained from the FEM calculation with those obtained from the proposed calculation method in the present paper on the thin-rimmed external spur gears with the pressure angles of α=20, 22.5, 25 degs. having 6 spokes respectively. With increasing pressure angle, the tensile and compressive tooth fillet and root stresses decrease a little. This is why the chordal tooth thickness on critical section increases and the nominal stresses of tooth decrease with increasing the pressure angle. But when the rim is thin, there is little influence of pressure angle on both tensile and compressive tooth

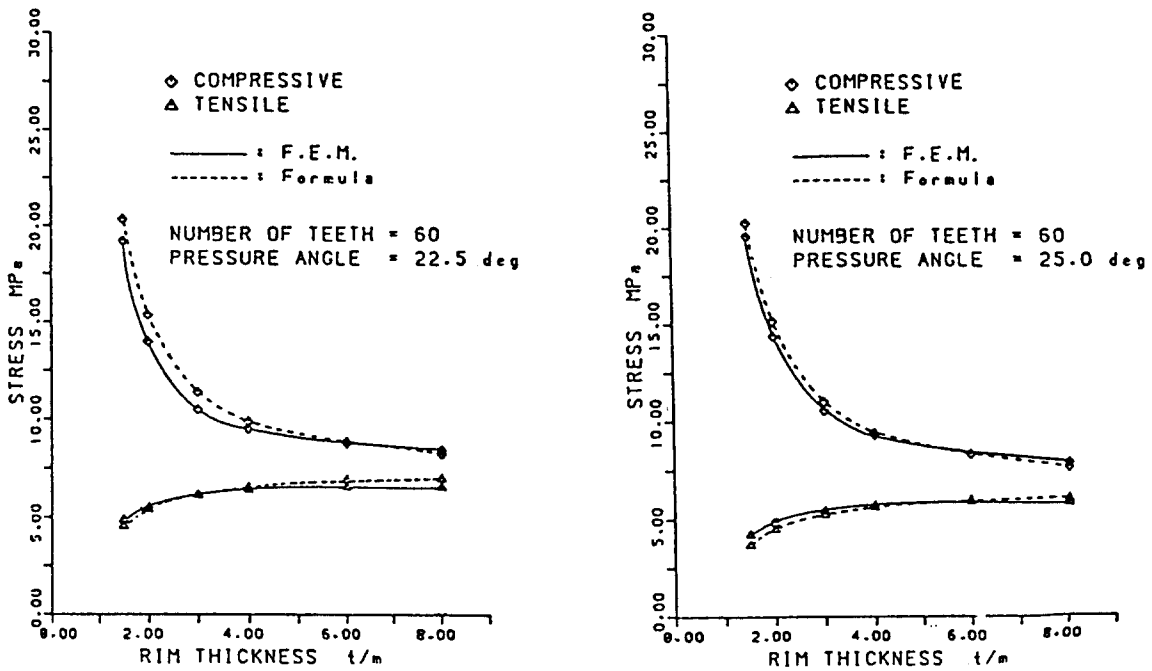

Fig.8 Comparison between tooth fillet and root stresses obtained by the present stress calculation method (dotted line) and those by the FEM calculation (line) according to the variation of pressure angle.

fillet and root stresses. This figure also shows that the calculated results by the present calculation method have good agreement with those by the FEM calculation, especially when the pressure angle becomes higher.

6.2 For a thin-rimmed internal gear fixed by bolts

The tooth fillet and root stress values between measured and calculated values were compared when an internal gear is fixed by bolts. The test internal gear for tooth fillet and root stress measurements by strain survey investigations is a standard addendum spur gear of module m=4㎜, α=20deg., z_i=66, h=2.25m, b=8㎜, made of SM45C(carbon steel of 0.45% carbon content). The rim thicknesses are four : 27㎜(6.75m), 18㎜ (4.5m), 12㎜(3m), and 8㎜(2m). An internal gear of t=27㎜ was at first used for stress measurements and then the rim thickness was decreased step by step to 18㎜, 12㎜, 8㎜. For the case when the internal gear mating with three planetary gears is fixed by three or six bolts, the fillet stresses at the point of θ=45deg. tangent to the fillet curve of the loaded tooth and the root stresses at the centers of bottoms of tooth spaces of the loaded and unloaded teeth over the whole internal gear were measured using strain gage of 0.5㎜ length. The load was applied on the tip of the central tooth between the fixing bolts

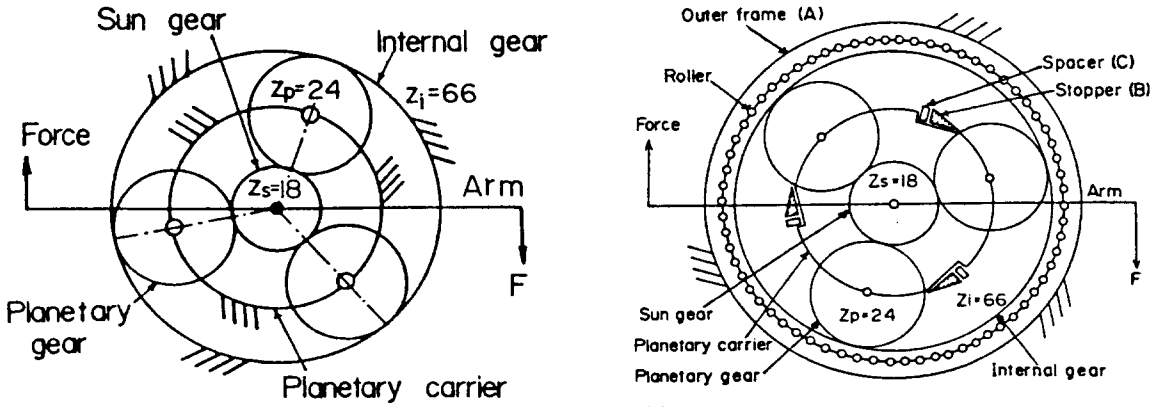

(a) When an internal gear is fixed by bolts

(b) When an internal gear is supported by rollers cpinned coupling

Fig.9 Schema of test rig.

under a single tooth pair meshing using a statically loading apparatus of an epicyclic gear train construction, as shown in Fig. 9(a).

This test rig is a simple planetary epicyclic gearing with three planetary gears and has an arm for loading. The rotational movement of the planetary carrier and the internal gear is fixed, and the torque applied on the arm is transmitted from a sun gear shaft to a sun gear, to planetary gears, and then to internal gear teeth. The point at which the planetary gear teeth mesh with the internal gear teeth can be selected by adjusting the spacer between the planetary carrier and the internal gear to change the relative rotational position between the two. In order to get uniform load distribution on every planetary gear, a sun gear is floatingly supported : The sun gear shaft has a bearing only at the joint of the loading arm.

Fig. 10 shows the effect of rim thickness on the tooth fillet stresses and also shows the comparison among the fillet stresses of a loaded tooth obtained by measurements, those by the FEM calculations, and those by the approximate calculation method developed in the present research. With decreasing rim thickness, the stress values increase on both the tension and compression sides of the loaded tooth, and the increasing rate on the compression side is remarkably high, particularly in the case when the internal gear is fixed by three bolts. It is recognized from this figure that the measured values, the FEM calculated values and the values calculated by the present method show fairly good agreement : The measured stress values on the compression side coincide well with both calculated values, but on the tension side the measured stress values take somewhat smaller values than both calculated values, especially in the region where the rigidity of rim becomes weaker. This phenomenon is clearly seen in Fig. 10(b) in the region of smaller rim thickness : When the internal gear is fixed by three bolts, there is a little difference between stress values by the present calculation method and by measurements. The cause of

this difference is considered as follow : This calculation method does not consider the influence that the loading angle ω at the tip of the tooth and the loading position would be actually somewhat changed in experiments owing to the deformation of rim and the deflection of the tooth. The fact could be also a cause of the difference that this calculation is carried out under the assumption of all the displacements including rotational displacement at the positions corresponding to the fixing bolts being zero.

Fig. 11 compares the measured stress distribution of root stresses at the bottoms of the tooth spaces of the loaded and unloaded teeth over 1/3 of the span of an internal gear with those obtained by the present calculation method for various rim thickness under fixing the internal gear by three bolts. The measured stress values and those by the present calculation method show fairly good agreement, and the accuracy of this calculation method is considered to be fairly high for stress distribution over the whole span of gear rim, even at the loaded and/or unloaded teeth. It is found from this figure that the stress values increase on both the tension and compression sides with reducing rim thickness : On the tension side as the rim becomes thinner, a larger root stress occurs

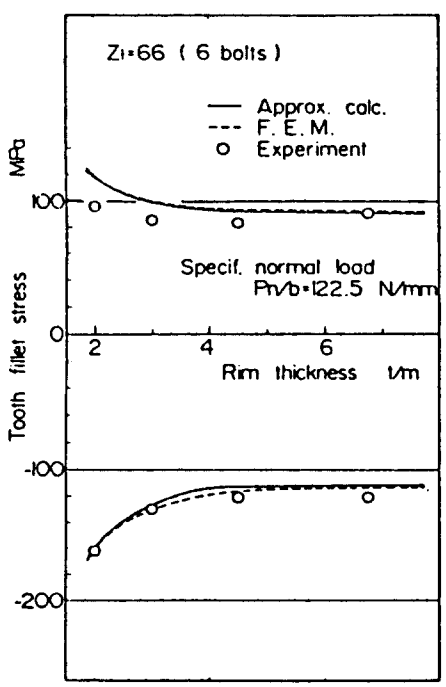

(a) Internal gear fixed by 6 bolts

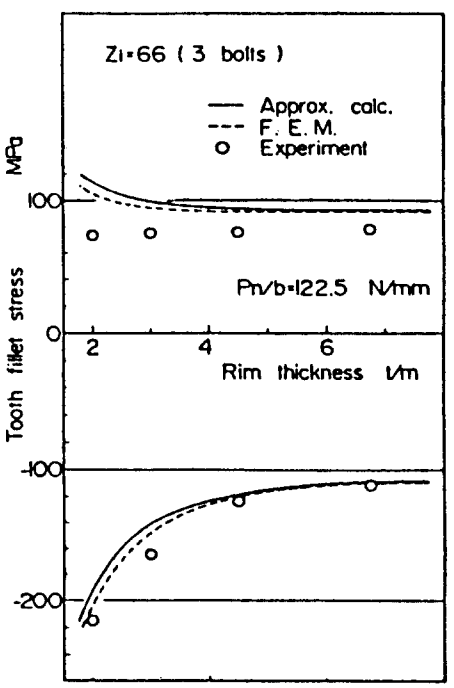

(b) Internal gear fixed by 3 bolts

Fig.10 Fillet stresses of a loaded tooth of internal gear fixed by bolts

at the bottom of a tooth space at some distance from the loaded tooth than at the fillet and bottom of tooth space of the loaded tooth, but on the compression side the largest root stress occurs always at the bottom of the tooth space of the loaded tooth in spite of the change of rim thickness.

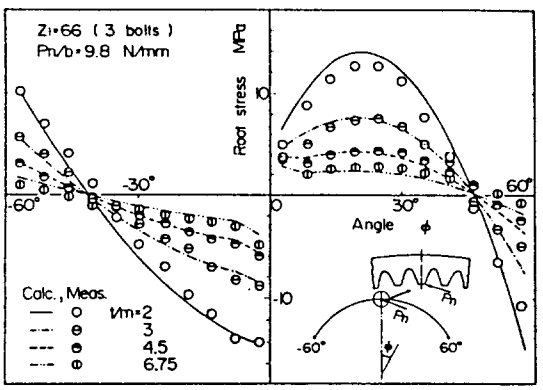

Fig.11 Root stresses at bottoms of tooth spaces over 1/3 of the span of internal gear fixed by bolts

6. 3 For a thin-rimmed internal gear supported by rollers

Internal gear is commonly supported by geared coupling teeth on the outer periphery of an internal gear, especially in an epicyclic gearing, and the stress analysis of such an internal gear is necessary. There are, however, some difficulties with the basic research in regard to choosing arbitrary combinations of rim thickness and the phase difference between internal and external gear teeth, that is, the relation between the angular position of the external teeth of geared coupling and that of internal gear teeth : They cannot be independently chosen because of the relation between module and number of teeth in the internal gear and geared coupling. A method to support an internal gear by pinned coupling is therefore employed in this experiment : With pinned coupling there is not such a difficult problem and the supporting condition of the internal gear is very similar to geared coupling. Pinned coupling is a supporting method of the internal gear by rollers inserted in holes between the outer frame(A) and the internal gear as shown in Fig. 9(b). The number of roller holes is 66, which is selected as the same number of in-

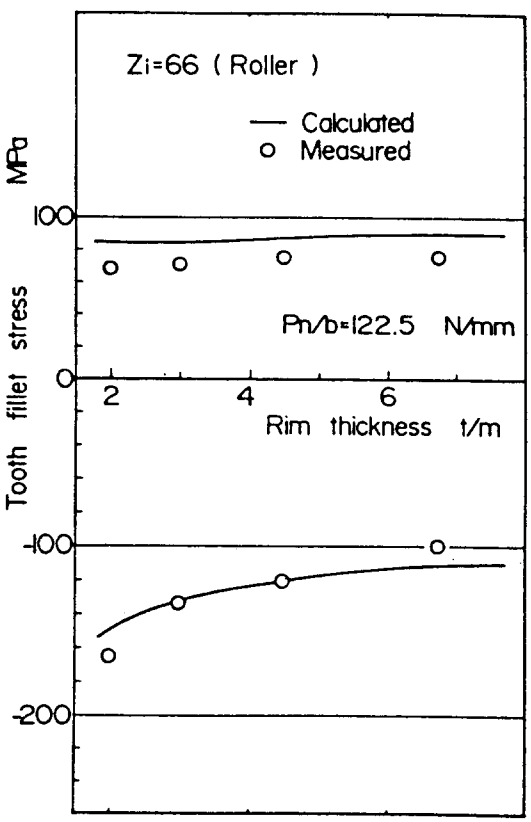

Fig.12 Comparison between measured and calculated fillet stresses of a loaded tooth when an internal gear is supported by rollers

ternal gear teeth. The roller holes are located just behind the teeth of the internal gear. The diameter of a roller hole is chosen to be 8. 25 mm, a little larger than the diameter of an 8mm roller.

The test internal spur gears used for stress measurements by strain survey investigations have the same dimensions as those of the bolt fixing test gears, except the dimensions concerning to the pinned coupling.

Fig. 12 shows the comparison between the measured fillet stresses of a loaded tooth and the calculated values by this calculation method, when the load is applied on the tip of the tooth under a single tooth pair meshing. This figure shows the tendency that stresses on the tension side decrease slightly but those on the compression side increase somewhat as the rim becomes thinner. When the rim thickness is two times of module (t=2m), the stress on the compression side becomes almost two times larger than the stress on the tension side. The reason for this phenomenon

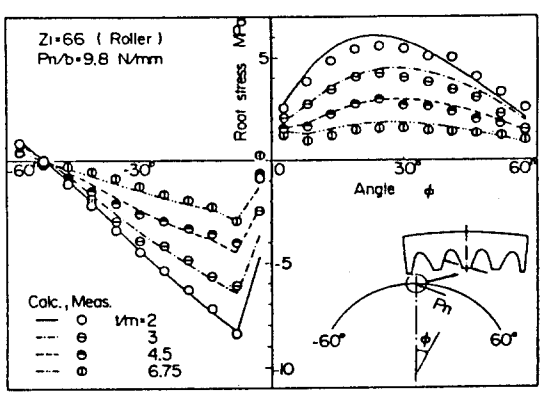

Fig.13 Root stresses at bottoms of tooth spaces over 1/3 of the span of internal gear under double tooth pair meshing when an internal gear is supported by rollers

is the same as in the case when an internal gear is fixed by bolts : The increase of rim deformation induces the increase of compressive stress component by rim bending at the fillet of a loaded tooth when the rim thickness decreases. The measured stress values and the calculated stress values show fairly good agreement. The cause of some small differences between measured and calculated stress values is thought to be the changes of the loading position and the loading angle owing to deformations of the rim and tooth of the internal gear in the actual stress measurement, which is the same reason as the former case when internal gear is fixed by bolts.

Fig. 13 shows the measured and calculated root stresses at the bottoms of tooth spaces over 1/3 of the span of an internal spur gear under a double tooth pair meshing. The measured and calculated stress values are found to show fairly good agreement. In this case when the internal gear is supported by rollers, the changing characteristics of the stresses owing to change of rim thickness are the same as for the case of an internal gear fixed by bolts. A big differnece between Fig. 11 and Fig. 13 is that the root stress at the first minus position of ϕ becomes much smaller in Fig. 13 than in Fig. 11, which is the result of a double tooth pair meshing for the case in Fig. 13 : This root position of stress measurement is between two loaded teeth, and the compessive and tensile stresses here compensate to each other.

In addition, it is seen that the stress state at tooth fillet and root areas of thin-rimmed spur gears becomes alternating stress state, as Drago[8, 9, 14] and Arai[5] pointed out.

The magnitude and stress state of the alternating stress distribution at tooth fillet and root areas, which becomes a big problem in a fatigue strength, are easily obtained by this calculation method.

7. Conclusions

(1) The approximation formulae to clculate the tooth fillet and root stresses of a thin-rimmed rack[1] are applied to the stress calculation of thin-rimmed external and internal spur gears. Here a general method to calculate the nominal stresses at the cross section of the rim of such thin-rimmed gears under consideration of rim dimensions and of supporting conditions of the rim is shown, which is necessary to execute this calculation.

(2) The stress values at the tooth fillet and root areas of thin-rimmed spur gears have shown good agreement between the stress values obtained from this calculation method and those from the FEM calculations and also from the measured stresses by the strain survey investigation. Also the state of stresses at tooth fillet and root areas in the thin-rimmed external and internal gears has become clear. The reliability of the stress values and stress state at tooth fillet and root areas of such thin-rimmed spur gears, calculated by the proposed stress calculation method developed in this work is admitted as the same as that by the FEM calculation. This calculation method will therefore contribute a great deal to the bending strength design of thin-rimmed spur gears.

References

(1) Chong, T.H., and Kubo, A., "Simple Stress Formulae for a Thin-Rimmed Spur Gear(Part 1 : Derivation of Approximation Formulat for Tooth Fillet and Root Stresses)", Trans. ASME., Journal of Mechanisms, Transmissions, and Automation in Design, Vol. 107, 1985-9, PP. 406-411.

(2) Chong, T.H., et al., "Bending Stresses of Internal Spur Gear", Bull. Japan Soc. Mech. Engrs., Vol. 25, No. 202, 1982, pp. 679-686.

(3) Hidaka, T., et al., "Effect of Rim Thickness and Number of Teeth of Internal Spur Gear on Bending Strength", Trans. Japan Mech. Engrs., (in Japanese), Vol. 49, No. 441, 1983, pp. 803-810.

(4) Chong, T.H., and Kubo, A., "Simple Stress Formulae for a Thin-Rimmed Spur Gear (Part 2 : Tooth Fillet and Root Stress Calculation of a Thin-Rimmed Internal Spur Gear)", Trans. ASME., Journal of Mechanisms, Transmissions, and Automation in Design, Vol. 107, 1985 -9, pp. 412-417.

(5) Arai, N., et al., "Research on Bending Strength Properties of Spur Gears", Bull, Japan Soc. Mech. Engrs., Vol. 24, No. 195, 1981, pp. 1642-1649.

(6) Oda, S., et al., "Stress Analysis of Thin Rim Spur Gears by Finite Element Method", Bull, Japan Soc. Mech. Engrs., Vol. 24, No. 193, 1981-7, pp. 1273

-1280.

(7) Chong, T. H., et al., "Bending Stresses of Internal Spur Gear", Bull. Japan Soc. Mech. Engrs., Vo. 25, No. 202, 1982-4, pp. 679-686.

(8) Drago, R. J., and Pizzigati, G. A., "Some Progress in the Accurate Evaluation of Tooth Root and Fillet Stresses in Lightweight, Thin-Rimmed gears", AGMA paper 229. 21, AGMA Fall Technical Meeting, Washington, D. C., 1980-10.

(9) Drago, R. J., and Lutthans, R. V., "An Experimental Investigation of the Combined Effects of Rim Thickness and Pitch Diameter on Spur Gear Tooth Root and Fillet Stresses", AGMA paper 229. 22, AGMA Fall Technical Meeting, Toronto, 1981-10.

(10) Sayama, T., et al., "Root Stresses and Bending Fatigue Strength of Welded Structure Gears", Proc. Int. Symp. Gearing and Power Transmissions, Tokyo, Vol. 1, 1981-8, p. 459.

(11) Hanna, H. A. M., "Stress Distribution Around Geared Rim", Proc. Int. Symp. Gearing and Power Transmissions, Tokyo, Vol. 2, 1981-8. p. 189.

(12) Dinovich, M. Ya. and Sholomov, N. M., "Stress Concentrations in Racks and on the Rims of Spur Gears", Russian Engng. Journal Vol. 57-3, 1977, p. 8.

(13) Dolgopolov, V. V., et al., "Stress in Planet Gears with a Thin Rim", Russian Engng. Journal Vol. 52-9, 1972, p. 6.

(14) Drago, R. J., "An Improvement in the Coventional Analysis of Gear Tooth Bending Fatigue Strength", AGMA paper P229. 34, AGMA Fall Technical Meeting, New Orleans, La., 1982-10

(15) Sayama, T., and Umezawa, K., "Study on Welded Structure Gear (12th report : Calculation Method of Fillet Stress on Thin Rim Gears with Center Web), Trans. Japan Soc. Mech. Engrs. (in Japanese), Series C, Vol. 52, No. 474, 1986, pp. 770-774.

(16) Oda, S. and Miyachika, K., "Practical Formula for True Stress of Internal Spur Gear Tooth", Bull. Japan Soc. Mech. Engrs., Vol. 29, No. 252, 1986, pp. 1934-1939.

(17) Sinkevich, Yu. B. and Sholomov, M. M., "Effect of Toothed-Ring Geometry on the Stiffness of its Rim", Russian Engng. Journal, Vo. 51-6, 1971, p. 25.

(18) Dinovichi, M. Ya., "Rigidity of the Toothed Rim on Spur Gears", Russian Engng. Journal, Vol. 55-6, 1975, p. 26.